*Int. J. Solids Structures*, 1976, Vol. 12, pp. 185–201. Pergamon Press. Printed in Great Britain

# AN ANALYSIS OF THE IMPERFECTION SENSITIVITY OF SQUARE ELASTIC-PLASTIC PLATES UNDER AXIAL COMPRESSION

ALAN NEEDLEMAN†‡
Department of Mathematics, Massachusetts Institute of Technology, Cambridge, MA 02139, U.S.A.

and

VIGGO TVERGAARD
Department of Solid Mechanics, The Technical University of Denmark, Lyngby, Denmark

(*Received* 30 *April* 1975)

**Abstract**—For a simply supported elastic-plastic square plate under axial compression the post-bifurcation behaviour and the sensitivity to initial imperfections are investigated. An exact asymptotic expansion is given for the initial post-bifurcation behaviour of a perfect plate compressed into the plastic range. The imperfection sensitivity is studied through an asymptotic analysis of the behaviour of the hypoelastic plate that results from neglecting the effect of elastic unloading. The results of the asymptotic analyses are compared with results of a numerical incremental solution by means of a combined finite element—Rayleigh Ritz method. The paper considers the effect of different in-plane boundary conditions and the effect of various degrees of strain hardening.

## 1. INTRODUCTION

This paper is concerned with the postbuckling behaviour and imperfection sensitivity of simply supported square elastic-plastic plates. The plate material is taken to be strain hardening and characterized by a flow theory of plasticity with a smooth yield surface. Two types of in-plane boundary conditions are considered; one requires all four edges of the plate to remain straight throughout the loading history, the other leaves the edges unconstrained. In the elastic range, these in-plane boundary conditions play a crucial role in determining the initial postbuckling behaviour of the plate[1]. However, previous studies of elastic-plastic square plates[2–4], have not investigated the effects of in-plane boundary conditions on the postbuckling behaviour and imperfection sensitivity in the plastic range.

For bifurcation of the perfect plate in the plastic range Hutchinson's theory of postbuckling[5, 6] is employed to obtain an asymptotically exact description of the initial post-bifurcation behaviour. For the plate with a small initial curvature, compressed into the plastic range, there is, as yet, no general theory available that relates the behaviour of the imperfect structure to the postbuckling behaviour of the corresponding perfect structure, as is done in Koiter's general theory of elastic stability[7]. Here, an analysis that neglects elastic unloading is employed in an attempt to assess the imperfection sensitivity of simply supported square plates, when bifurcation of the perfect plate occurs in the plastic range. This analysis, approximate for the problems considered here, is based on that employed by Hutchinson and Budiansky[8] in their exact analysis of the postbuckling behavior of a cruciform column.

The post-bifurcation behaviour and imperfections sensitivity of elastic-plastic simply supported square plates are also determined numerically in an incremental fashion. The numerical procedure employed at each stage of the loading history is a combined finite element—Rayleigh Ritz method[9, 10]. The numerical results are compared with the analytical predictions.

## 2. PROBLEM FORMULATION

We consider square plates of length $a$ and thickness $h$. The displacements of the plate middle surface are denoted by $u_\alpha$§ and $w$, where $u_\alpha$ are the in-plane displacements and $w$ is the lateral displacement. Then with the usual approximations of von Kármán plate theory, the Lagrangian

†Partially supported by NSF Grant GP 22976.
‡Present address: Brown University, Div. of Engineering, Barus and Holley 7th Fl., Providence, RI 02912, U.S.A.
§In this paper Greek subscripts range from 1 to 2 and Latin subscripts range from 1 to 3.

strain increment tensor is given by,

$$\dot{\eta}_{\alpha\beta} = \dot{E}_{\alpha\beta} + x_3\dot{\kappa}_{\alpha\beta} \tag{1}$$

$$\dot{E}_{\alpha\beta} = \dot{e}_{\alpha\beta} + \frac{1}{2}(\dot{w}_{,\alpha}w_{,\beta} + w_{,\alpha}\dot{w}_{,\beta}) \tag{2a}$$

$$\dot{e}_{\alpha\beta} = \frac{1}{2}(\dot{u}_{\alpha,\beta} + \dot{u}_{\beta,\alpha}) \tag{2b}$$

$$\dot{\kappa}_{\beta\alpha} = -\dot{w}_{,\alpha\beta}. \tag{3}$$

Here, $x_3$ is the coordinate normal to the plate middle surface, $\dot{(\ )}$ denotes differentiation with respect to some monotonically increasing parameter that characterizes the loading history and $(\ ),\alpha$ denotes partial differentiation with respect to the inplane Cartesian coordinate $x_\alpha$.

The stress increments are related to the strain increments (1) by

$$\dot{\sigma}_{ij} = \mathscr{L}_{ijkl}\dot{\eta}_{kl}. \tag{4}$$

The 3-D tensor of moduli, $\mathscr{L}_{ijkl}$, has two branches. One corresponds to plastic loading, the other to elastic unloading. The elastic tensor of moduli, $\mathscr{L}^e_{ijkl}$, is taken to be isotropic so that

$$\mathscr{L}^e_{ijkl} = \frac{E}{1+\nu}\left[\frac{1}{2}(\delta_{ik}\delta_{jl} + \delta_{il}\delta_{jk}) + \frac{\nu}{1-2\nu}\delta_{ij}\delta_{kl}\right] \tag{5}$$

Where $E$ is Young's modulus, $\nu$ is Poisson's ratio and $\delta_{ij}$ is the Kronecker delta.

The theory of plasticity employed here is small strain $J_2$-flow theory with isotropic hardening for which the 3-D tensor of moduli (4) is given by

$$\mathscr{L}_{ijkl} = \mathscr{L}^e_{ijkl} - q\frac{s_{ij}s_{kl}}{\sigma_e^2} \tag{6}$$

where

$$s_{ij} = \sigma_{ij} - \frac{1}{3}\sigma_{kk}\delta_{ij}\,;\ \sigma_e = \left[\frac{3}{2}s_{ij}s_{ij}\right]^{1/2} \tag{7}$$

and

$$q = \begin{cases} 0, & \text{if } \sigma_e < Y \text{ or } \dot{\sigma}_e < 0 \\ \dfrac{3}{2}\dfrac{E}{1+\nu}\dfrac{1-E_t/E}{\frac{2}{3}(1+\nu)E_t/E + 1 - E_t/E}, & \text{if } \sigma_e = Y \text{ and } \dot{\sigma}_e \geq 0. \end{cases} \tag{8}$$

The tangent modulus, $E_t$, is the slope of the uniaxial stress-strain curve and $Y$, the flow stress, is the greater of the maximum value of $\sigma_e$ over the stress history and the initial yield stress, $\sigma_y$.

The representation of uniaxial stress-strain behaviour chosen is a piecewise power law with a well defined yield stress and continuous tangent modulus,

$$\frac{\epsilon}{\epsilon_y} = \begin{cases} \dfrac{\sigma}{\sigma_y}, & \text{for } \sigma < \sigma_y \\ \dfrac{1}{n}\left(\dfrac{\sigma}{\sigma_y}\right)^n + 1 - \dfrac{1}{n}, & \text{for } \sigma \geq \sigma_y \end{cases} \tag{9}$$

where $n$ is the strain hardening exponent and $\epsilon_y = \sigma_y/E$.

Since the plate is approximately in a state of plane stress, only the in-plane stresses enter into the constitutive relation. Thus,

$$\dot{\sigma}_{\alpha\beta} = L_{\alpha\beta\gamma\delta}\dot{\eta}_{\gamma\delta} \tag{10}$$

and the tensor of plane stress moduli is given by

$$L_{\alpha\beta\gamma\delta} = \mathscr{L}_{\alpha\beta\gamma\delta} - \frac{\mathscr{L}_{\alpha\beta 33}\mathscr{L}_{\gamma\delta 33}}{\mathscr{L}_{3333}}. \tag{11}$$

It is convenient to introduce the membrane stress tensor $N_{\alpha\beta}$ and the moment tensor $M_{\alpha\beta}$ where,

$$N_{\alpha\beta} = \int_{-h/2}^{h/2} \sigma_{\alpha\beta}\, dx_3, \qquad M_{\alpha\beta} = \int_{-h/2}^{h/2} \sigma_{\alpha\beta} x_3\, dx_3. \tag{12}$$

The incremental principle of virtual work now takes the form

$$\int_A [\dot{N}_{\alpha\beta}\delta\dot{e}_{\alpha\beta} + \dot{M}_{\alpha\beta}\delta\dot{\kappa}_{\alpha\beta} + \dot{N}_{\alpha\beta}w_{,\alpha}\delta\dot{w}_{,\beta} + N_{\alpha\beta}\dot{w}_{,\alpha}\delta\dot{w}_{,b}]\, dA = (EVW)^{\cdot} \tag{13}$$

where $(EVW)^{\cdot}$ is the increment of the external virtual work and $A$ is the area of the plate. Since the tensor of moduli possesses the symmetry $L_{\alpha\beta\gamma\delta} = L_{\gamma\delta\alpha\beta}$, the virtual work eqn (13) is the (weak) Euler equation of a variation principle for the displacement increment fields $\dot{u}_\alpha$ and $\dot{w}$. This principle is used as the basis for the numerical method that will be described subsequently.

In this study attention is confined to square plates simply supported on all four sides, i.e.

$$\begin{aligned} &\dot{w} = 0, \quad \dot{M}_{11} = 0 \quad \text{on} \quad x_1 = 0, a \\ &\dot{w} = 0, \quad \dot{M}_{22} = 0 \quad \text{on} \quad x_2 = 0, a \end{aligned} \tag{14}$$

and uniform compressive loading is applied in the $x_1$-direction.

Two sets of in-plane boundary conditions are considered. First all four edges are constrained to remain straight so that in Case I

$$\begin{aligned} &\dot{u}_1(0, x_2) = -\dot{u}_1(a, x_2) = \dot{U} \\ &\dot{u}_2(x_1, 0) = -\dot{u}_2(x_1, a) = -\dot{V} \end{aligned} \tag{15}$$†

and the constant edge displacement increments $\dot{U}$ and $\dot{V}$ are determined so that the following conditions for the edge tractions are satisfied

$$\int_0^a \dot{N}_{22}(x_1, 0)\, dx_2 = \int_0^a \dot{N}_{22}(x_1, a)\, dx_2 = 0 \tag{16a}$$

$$\dot{N}_{12} = 0 \quad \text{on} \quad x_1 = 0, a \quad \text{and} \quad x_2 = 0, a \tag{16b}$$

$$\int_0^a \dot{N}_{11}\, dx_2 \quad \text{prescribed at} \quad x_1 = 0, a. \tag{16c}$$

In the second case, the edges are unconstrained. Thus, in Case II (16b) holds together with

$$\dot{N}_{22}(x_1, 0) = N_{22}(x_1, a) = 0 \tag{17a}$$

$$\dot{N}_{11} \quad \text{prescribed at} \quad x_1 = 0, a. \tag{17b}$$

Both Cases, I and II, are compatible with a uniform uniaxial state of stress, so that in each case, one solution to the boundary value problem is

$$\sigma^0_{\alpha\beta} = -\lambda\delta_{1\alpha}\delta_{1\beta} \tag{18a}$$

†In the numerical computations it was often advantagous to prescribe $\dot{U}$ and then calculate the average traction. However, for uniformity of presentation it is convenient to consider the average traction to be the prescribed quantity.

or in terms of the membrane stress and moment tensors

$$N^0_{\alpha\beta} = h\sigma^0_{\alpha\beta}, \quad M^0_{\alpha\beta} = 0. \tag{18b}$$

Bifurcation from this solution first becomes possible when $\lambda = \lambda_c$ where

$$\lambda_c = \frac{E}{12}\left(\frac{\pi h}{a}\right)^2 \left[\frac{2}{1+\nu} + \frac{9+\dfrac{E_t}{E}(8\nu-1)}{(5-4\nu)-\dfrac{E_t}{E}(1-2\nu)^2}\right] \tag{19}$$

and the corresponding eigenmode displacement is

$$\overset{(1)}{w} = \pm h \sin\frac{\pi x_1}{a} \sin\frac{\pi x_2}{a}. \tag{20}$$

The eigenvalue (19) and eigenmode (20) apply for both Case I and Case II. However, as will be seen subsequently the in-plane boundary conditions can have a marked influence on the postbuckling behaviour of the plate.

## 3. ASYMPTOTIC ANALYSIS

In the elastic range ($\lambda_c < \sigma_y$), the initial postbifurcation behaviour of a simply supported square plate can be determined from Koiter's general theory of elastic stability [1, 7]. The initial postbifuration behaviour is stable in the sense that the plate can support applied stresses higher than $\lambda_c$.

For $\lambda_c > \sigma_y$, the initial postbifurcation behaviour is determined by means of Hutchinson's asymptotic theory of postbuckling in the plastic range [6], which extends the bifurcation analysis of Hill [11] into the post-bifurcation range. Denoting the amplitude of the eigenmode (20) by $\xi$ so that

$$w = \xi \overset{(1)}{w} + \cdots \tag{21}$$

the applied stress at bifurcation varies as

$$\lambda = \lambda_c + \lambda_1 \xi + \cdots \tag{22}$$

where the sign of $\overset{(1)}{w}$ is chosen so that $\xi$ is positive and

$$\lambda_1 = \left(\frac{\pi h}{a}\right)^2 E_t \frac{(1+\nu)}{(5-4\nu)-\dfrac{E_t}{E}(1-2\nu)^2}. \tag{23}$$

Here, the initial slope, $\lambda_1$, is uniquely determined by the requirement that plastic loading takes place through the plate except at one point where neutral loading occurs [6]. This slope is positive so that bifurcation takes place under increasing load in accord with Shanley's concept.

After bifurcation, a region of elastic unloading eminates from the point of neutral loading. The next term in the postbifurcation expansion for $\lambda$ takes into account the penetration of this region of elastic unloading into the plate and is proportional to $\xi^{4/3}$ [6], so that

$$\lambda = \lambda_c + \lambda_1 \xi + \lambda_2 \xi^{4/3} + \cdots \tag{24}$$

This expression is asymptotically exact for small $\xi$, the only approximation being that inherent in plate theory.

An explicit formula for $\lambda_2$ will not be given here, but we note that the only field quantities that enter into the determination of $\lambda_2$ are those associated with the prebifurcation solution (18) and

the eigenmode (20). Therefore, the nonlinear geometric terms do not enter into the postbifurcation expansion to the order given in (24). In particular this means that the inplane boundary conditions do not effect the value of $\lambda_2$ and, thus, the first three terms of (24) are identical for both sets of in-plane boundary conditions.

Since in all cases we find $\lambda_2 < 0$, the first three terms of (24) can be employed to estimate the value of the maximum support stress $\lambda_{max}$ and the corresponding bifurcation mode amplitude $\xi_{max}$. It must be emphasized that although (24) is an asymptotically exact expression, the values of $\lambda_{max}$ and $\xi_{max}$ obtained from the first three terms are not asymptotic in any sense, since the maximum occurs at a finite (perhaps small) value of $\xi$. Table 1 displays several results obtained from this initial postbifurcation analysis. In all cases the $\lambda_{max}$ is only slightly higher than $\lambda_c$.

In the plastic range, one would like to develop an asymptotic expansion about the bifurcation point that relates the behaviour of a slightly imperfect plate to the postbifurcation behaviour of the perfect plate as Koiter's[7] general theory relates the behaviour of a slightly imperfect elastic structure to the postbifurcation behaviour of a perfect one. However, for elastic-plastic structures such an analytical treatment of imperfection-sensitivity is made difficult by the fact that the maximum support load is attained at a limit point after finite bifurcation mode deflections and not at the bifurcation point as is the case for elastic structures[12]. Furthermore, for "symmetric" structures such as flat plates, it would be necessary to continue (24) beyond the first three terms in order to account for the geometric nonlinearities that play a crucial role in determining the elastic postbifurcation behaviour.

Table 1. Constants in plastic postbifurcation analysis for square plates

| h/a | n | $\sigma_y/E$ | $\nu$ | $\lambda_c/\sigma_y$ | $\lambda_1/\lambda_c$ | $\lambda_2/\lambda_c$ | $\lambda_{max}/\lambda_c$ | $\xi_{max}$ |
|---|---|---|---|---|---|---|---|---|
| 0.031 | 3 | 0.00337 | 0.3 | 1.025 | 0.931 | -6.018 | 1.0004 | 0.00156 |
| 0.031 | 10 | 0.00337 | 0.3 | 1.015 | 0.857 | -4.515 | 1.0006 | 0.00288 |
| 0.035 | 3 | 0.00337 | 0.3 | 1.259 | 0.632 | -1.854 | 1.0026 | 0.0167 |
| 0.035 | 10 | 0.00337 | 0.3 | 1.196 | 0.206 | -0.397 | 1.003 | 0.0594 |

Here, we will attempt an assessment of the imperfection-sensitivity of simply supported square plates by an analysis that ignores elastic unloading. The constitutive eqns (4) are employed, but the plastic loading branch of the tensor of moduli is taken to be active regardless of the sign of $\dot{\sigma}_e$. Thus, our analysis is strictly applicable for a hypoelastic but *not* for an elastic-plastic plate. For such a hypothetical hypoelastic plate, the difficulties mentioned previously disappear. The postbifurcation analysis for a perfect plate proceeds along the same general lines as the analysis for elastic plates. The maximum support load of a perfect plate, if there is one in the vicinity of the bifurcation point, is the bifurcation load and an asymptotic expression can be found that relates the maximum support load of a plate with a small imperfection to the bifurcation load of the perfect plate. In this aspect of the analysis there is a significant difference between the analysis for the path dependent hypoelastic material and that for an elastic material. This analysis is a generalization to the full von Kármán plate equations of the analysis given recently by Hutchinson and Budiansky[8] and is presented in the Appendix. Here, only the main results are stated.

Attention is confined to imperfections in the shape of the bifurcation mode (20) and the amplitude of the imperfection is donoted by $\bar{\xi}$. For $\lambda < \lambda_c$, the lowest order effect of the imperfection on the magnitude of the lateral deflection $\xi$, is found by a regular perturbation analysis to be

$$\xi = \bar{\xi}(1 - \lambda/\lambda_c)^{-\Psi} p(\lambda) \tag{25}$$

where $\Psi$ is a positive constant greater than or equal to unity, given by (A31), and $p(\lambda)$ is a function of $\lambda$, that is finite at $\lambda_c$. For an elastic material, even a nonlinear one, $\Psi = 1$.

In the vicinity of $\lambda_c$, a singular perturbation analysis gives $\lambda$ as the following function of $\xi$

$$\lambda = \lambda_c + \lambda_2^{he}\xi^2 + c\bar{\xi}^{(2\Psi+1/\gamma\Psi)}\xi^{-(1/\Psi)}. \tag{26}$$

Here, $\Psi$ is the same constant appearing in (25), $c$ and $\gamma$ are undetermined by the analysis and $\lambda_2^{he}$ is obtained as outlined in the Appendix and requires the solution of an auxiliary boundary value problem. It is in the solution of this boundary value problem that the in-plane boundary conditions play a crucial role in determing the value of $\lambda_2^{he}$.

For $\lambda$ near $\lambda_c$, (25) may be rewritten in the form (A34) and matching (25) and (26) determines $c$ and $\gamma$, namely

$$c = -\lambda_c(p(\lambda_c))^{1/\Psi}, \qquad \gamma = 2\Psi + 1. \tag{27}$$

If $\lambda_2^{he} < 0$, a maximum support stress, $\lambda_{max}$, occurs according to (26), which is given by

$$\frac{\lambda_{max}}{\lambda_c} = 1 - \mu(\xi)^{2/(2\Psi+1)} \tag{28}$$

where

$$\mu = -\frac{\lambda_2^{he}}{\lambda_c}(2\Psi+1)\left(-\frac{2\Psi\lambda_2^{he}}{\lambda_c}\right)^{-2\Psi/(2\Psi+1)} p(\lambda_c)^{2/(2\Psi+1)}. \tag{29}$$

In Table 2, the results obtained from the hypoelastic postbifurcation analysis are given for the same values of the parameters employed in the examples in Table 1 The most interesting predictions are that, for $n = 3$, the initial postbifurcation behaviour is stable for three of the four examples, while for $n = 10$, the initial postbifurcation behaviour is unstable for all cases considered and for the example with $h/a = 0{\cdot}035$ nearly independent of the in-plane boundary conditions. We emphasize that, although the results displayed in Table 2 are asymptotically exact for the hypoelastic plate, they are only approximate for an elastic-plastic plate and are in no sense asymptotic.

Finally, we note that when $\lambda_c < \sigma_y$, $\lambda_2^{he}$ reduces to the appropriate value for a linear elastic plate $\lambda_2^e$. The auxiliary boundary value problem for the linear elastic plate was solved by the same numerical method employed in the hypoelastic calculation to obtain for $\nu = 0{\cdot}3$, $\lambda_2^e/\lambda_c = 0{\cdot}343$ with the constrained in-plane boundary condition (Case I) and $\lambda_2^e/\lambda_c = 0{\cdot}179$ with the unconstrained in-plane boundary condition (Case II). For Case I, the exact value is $\lambda_2^e/\lambda_c = 0{\cdot}341$ with $\nu = 0{\cdot}3$, see e.g.[17].

## 4. NUMERICAL METHOD AND RESULTS

The numerical results to be presented here are obtained by an incremental method based on the variational eqn (13). An initial imperfection of the form

$$\bar{w} = \bar{\xi}\overset{(1)}{w} \tag{30}$$

is specified where $\overset{(1)}{w}$ is the bifurcation mode (20) and $\bar{\xi}$ denotes the imperfection amplitude. All

Table 2. Constants in hypoelastic postbifurcation analysis for square plates with $\sigma_y/E = 0{\cdot}00337$ and $\nu = 0{\cdot}3$. The numbers in the last column refer to in-plane boundary conditions

| h/a | n | $\lambda_c/\sigma_y$ | $\lambda_2^{he}/\lambda_c$ | $\Psi$ | $2/(2\Psi+1)$ | $\mu$ | |
|---|---|---|---|---|---|---|---|
| 0.031 | 3 | 1.025 | +0.153 | 1.0318 | 0.6528 | – | I |
| 0.031 | 3 | 1.025 | +0.014 | 1.0318 | 0.6528 | – | II |
| 0.031 | 10 | 1.015 | -0.039 | 1.0601 | 0.6410 | 0.359 | I |
| 0.031 | 10 | 1.015 | -0.185 | 1.0601 | 0.6410 | 0.591 | II |
| 0.035 | 3 | 1.259 | +0.030 | 1.4133 | 0.5227 | – | I |
| 0.035 | 3 | 1.259 | -0.048 | 1.4133 | 0.5227 | 0.440 | II |
| 0.035 | 10 | 1.196 | -0.303 | 3.9557 | 0.2244 | 0.326 | I |
| 0.035 | 10 | 1.196 | -0.308 | 3.9557 | 0.2244 | 0.327 | II |

results given here for a "perfect" plate are actually the results of a calculation using a small imperfection, $\bar{\xi} = 10^{-4}h$. At each stage of the loading history, an approximate solution of (13) is obtained by the combined Rayleigh Ritz-finite element procedure employed in [9, 10], which is a modified version of a method originated by Kawai and Ohtsubo [13, 3]. The increment of lateral displacement $\dot{w}$, is expanded in terms of smooth functions $\hat{w}^j$ as in the standard Rayleigh Ritz method

$$\dot{w} = \sum_{j=1}^{N} \dot{\xi}_j^* \hat{w}^j. \tag{31}$$

The corresponding in-plane displacements $\hat{u}_\alpha^j$ are determined by a finite element calculation. The plate is divided into rectangular elements and the functions $\hat{u}_\alpha^j$ are expanded in term of cubic "serendipity" elements (Zienkiewicz [14]).

First (13) is solved for the in-plane displacement field $\hat{u}_\alpha^j$ corresponding to each $\hat{w}^j$. In addition, for Case I, two in-plane modes $\hat{u}_\alpha^{N+1}$ and $\hat{u}_\alpha^{N+2}$ are computed corresponding to uniform prescribed edge displacements in $x^1$- and $x^2$-direction, respectively, and, for Case II, one in-plane mode $\hat{u}_\alpha^{N+1}$ is computed corresponding to the prescribed edge loads. Thus, the in-plane displacement functions are given by,

$$\hat{u}_\alpha = \sum_{j=1}^{N+M} \dot{\xi}_j^* \hat{u}_\alpha^j \qquad M = 1 \quad \text{or} \quad 2. \tag{32}$$

Equations (31) and (32) now give the trial functions employed in the Rayleigh Ritz method.

In the solution of the Rayleigh Ritz problem, we avoid difficulties around the maximum load by always prescribing that one of the $N+M+1$ parameters, $\dot{\xi}_1^*, \dot{\xi}_2^*, \ldots, \dot{\xi}_{N+M}^*, \dot{\lambda}$ that is numerically largest in the previous increment and then solving (13) for the remaining $N+M$ parameters. Once the $\dot{\xi}_j^*$ have been determined the slightly corrected increments, $\dot{\xi}_j$, are found by using the curvatures of the function $\xi_j(\lambda)$, which are numerically estimated using the slopes of the previous increment.

Here, the assumed functions $\hat{w}_j$ are taken of the form

$$\hat{w}^j = h \sin \frac{\pi j_1 x}{a} \sin \frac{\pi j_2 x}{a}. \tag{33}$$

Due to symmetries the computations to be presented here are carried out for only one quarter of the plate and $j_1$ and $j_2$ are taken to be odd integers. Furthermore, it was found to be sufficient only to consider $j_1$ and $j_2$ ranging from 1 to 3. Including higher order modes has no appreciable effect.

The quarter of the plate considered is divided into 4 elements and 16 point Gaussian quadrature is used to evaluate in-plane integrals while a 7 point Simpson's rule is employed through the thickness.

The active branch of the tensor of moduli (11) is determined at each integration point as follows. If the stress state is on its current yield surface, the plastic loading branch is taken to be active. Then, if $\dot{\sigma}_e$ turns out to be negative the elastic unloading branch is taken to be active in the next increment. This procedure is only accurate if small increments are used and if the transition from loading to unloading occurs only once or twice during the loading history.

Figures 1 and 2 display results for cases in which bifurcation of the perfect plate occurs in the plastic range. In both cases, $h/a = 0{\cdot}035$, $\nu = 0{\cdot}3$ and $\sigma_y/E = 0{\cdot}00337$; in Fig. 1 $n = 10$ and $\lambda_c/\sigma_y = 1{\cdot}196$ while in Fig. 2 $n = 3$ and $\lambda_c/\sigma_y = 1{\cdot}259$. Even though bifurcation occurs well into the plastic range, the bifurcation predictions of $J_2$-flow theory and those of the simplest deformation theory, $J_2$-deformation theory, do not differ greatly. In Fig. 1 with $n = 10$ the discrepency is 5·8% while in Fig. 2 with $n = 3$ it is 2·3%.

The next two figures, Figs. 3 and 4, display results for plates with $h/a = 0{\cdot}031$, $\nu = 0{\cdot}3$ and $\sigma_y/E = 0{\cdot}00337$ in which bifurcation of the perfect plate occurs just after plastic yielding. In this situation, there is virtually no discrepency between the bifurcation predictions of $J_2$-flow theory and those of $J_2$-deformation theory. In Fig. 3, $n = 10$, and $\lambda_c/\sigma_y = 1{\cdot}015$ while in Fig. 4 $n = 3$ and $\lambda_c/\sigma_y = 1{\cdot}025$.

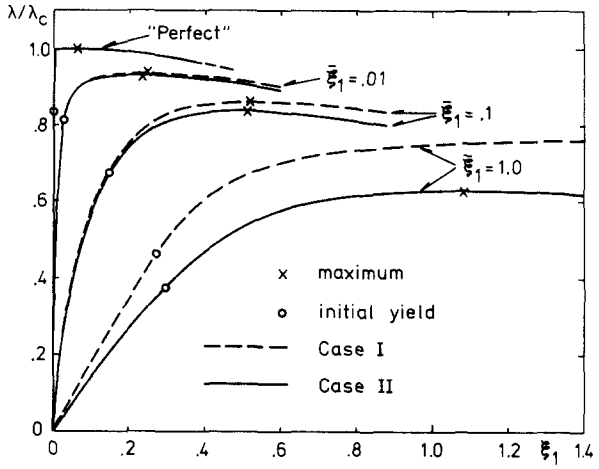


Fig. 1. Load vs buckling mode displacement for square plate ($\sigma_y/E = 0{\cdot}00337$, $h/a = 0{\cdot}035$, $n = 10$, $\nu = 0{\cdot}3$).

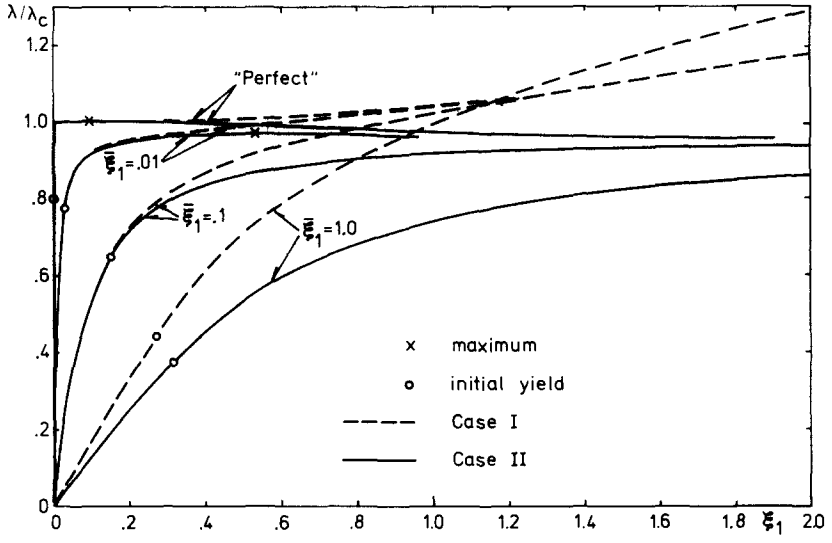


Fig. 2. Load vs buckling mode displacement for square plate ($\sigma_y/E = 0{\cdot}00337$, $h/a = 0{\cdot}035$, $n = 3$, $\nu = 0{\cdot}3$).

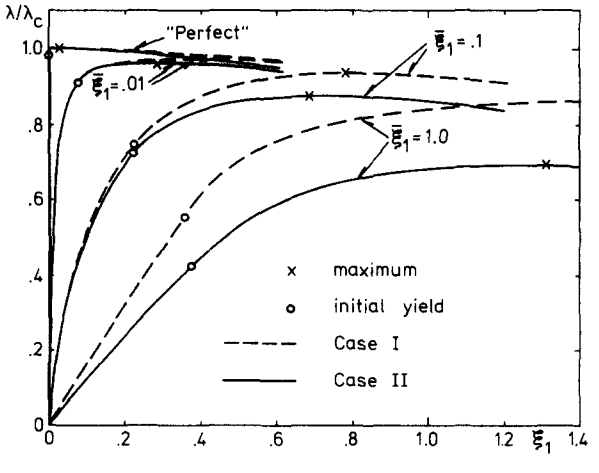


Fig. 3. Load vs buckling mode displacement for square plate ($\sigma_y/E = 0{\cdot}00337$, $h/a = 0{\cdot}031$, $n = 10$, $\nu = 0{\cdot}3$).

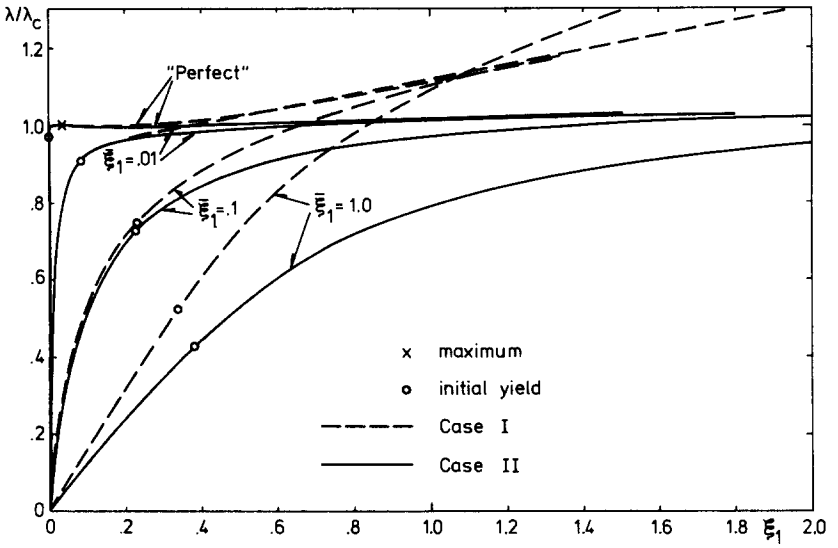


Fig. 4. Load vs buckling mode displacement for square plate ($\sigma_y/E = 0{\cdot}00337$, $h/a = 0{\cdot}031$, $n = 3$, $\nu = 0{\cdot}3$).

For the perfect plates, the behaviour in the immediate vicinity of the bifurcation point is described by (24) in that bifurcation takes place under increasing load and the curvature of the load deflection curve is large and negative. Furthermore, in the immediate vicinity of the bifurcation point, the initial postbifurcation behaviour is independent of the boundary conditions.

In Fig. 1, where $n = 10$, the maximum support load and the buckling deflection, $\xi$, at the maximum load are seen to be in good agreement with the results in Table 1. After the maximum load point, the load falls of rapidly. The postbucklong behaviour of the perfect plate is virtually identical for both sets of in-plane boundary conditions, as is the behaviour of a plate with a small imperfection, $\bar{\xi} = 0{\cdot}01$. On the other hand as the initial imperfection amplitude is increased the effect of the in-plane boundary conditions becomes significant. For the largest imperfection amplitude considered here, $\bar{\xi} = 1{\cdot}0$, the plate with the constrained boundary conditions has a maximum support load about 25% higher than the one with the unconstrained in-plane boundary condition.

In Fig. 2, where $n = 3$, the postbifurcation behaviour of the perfect plate depends crucially on the in-plane boundary conditions. With the unconstrained in-plane boundary conditions the load reaches a maximum and thereafter decreases monotonically, whereas with the constrained boundary condition the load continues to rise. Here, the mode amplitude, $\xi_{max}$, obtained from (24) is considerably smalller than the numerical value obtained with the unconstrained boundary condition. The load-deflection behaviour of the plate with an initial imperfection also depends crucially on the in-plane boundary conditions. An imperfect plate with the constrained in-plane boundary condition can support loads in excess of the bifurcation load, while plates with the unconstrained boundary condition exhibit a mild imperfection sensitivity.

In Fig. 3, where $n = 10$, the load on the perfect plates reaches a maximum shortly after bifurcation, and thereafter decreases monotonically. Compared with the example in Fig. 1, where bifurcation of the perfect plate occurred further into the plastic range, the effect of the in-plane boundary conditions shows up much sooner here. Also, even for an initial imperfection amplitude of $\bar{\xi} = 0{\cdot}01$, the effect of the in-plane boundary conditions on the load deflection behaviour of the plate is noticable. This effect increases with the amplitude of the initial imperfection. Note that in Fig. 3, for each initial imperfection amplitude considered, the imperfection sensitivity is less than for the corresponding example in Fig. 1.

In Fig. 4, where $n = 3$, the load-buckling deflection curves for the perfect plates reach a maximum, decrease, reach a minimum and thereafter increase. For both sets of in-plane boundary conditions no imperfection sensitivity is exhibited.

Computations have also been carried out for a plate that bifurcates elastically at a stress 3% below $\sigma_y$. The results for $n = 10$ and $n = 3$ differ very little from those of Figs. 3 and 4, except that the postbifurcation behaviour of the perfect plate is initially elastic untill yielding starts at $\xi_1 \simeq 0{\cdot}05$. To compare with the results of Mayers and Budiansky [2] for the constrained in-plane

condition, Case I, a few computations were also made with $n = 7{\cdot}25$. In agreement with Ref. [2] a stable postbuckling behaviour was found for Case I, and furthermore it was found that Case II is somewhat imperfection-sensitive. The present results show that square elastic-plastic plates are considerably less imperfection-sensitive than circular elastic-plastic plates [15].

The numerical results displayed in Figs. 1–4 shall now be compared with the predictions of the asymptotic analysis with elastic unloading neglected. The relevant constants obtained by means of this hypoelastic analysis are given in Table 2. In Table 3 the asymptotic predictions of maximum loads and corresponding mode amplitudes for imperfect hypoelastic plates are compared with the numerical results for elastic-plastic plates. For $n = 10$ and $h/a = 0{\cdot}035$ (Fig. 1) the asymptotic analysis indicates that the postbifurcation behaviour and the behaviour of a plate with a small initial imperfection is virtually independent of the in-plane boundary conditions in agreement with the numerical results. For $n = 3$ and $h/a = 0{\cdot}035$ (Fig. 2) the hypoelastic analysis is also in qualitative agreement with the numerical results. For the constrained in-plane boundary conditions, this analysis predicts the stable initial postbifurcation behaviour and corresponding lack of imperfection-sensitivity displayed in Fig. 2. On the other hand for the unconstrained in-plane boundary condition, (28) gives an imperfection-sensitivity in agreement with the numerical results. For $n = 10$ and $h/a = 0{\cdot}031$ (Fig. 3) the asymptotic results agree with the numerical results in predicting imperfection-sensitivity for both sets of in-plane boundary conditions. Finally for $n = 3$ and $h/a = 0{\cdot}031$ (Fig. 4) $\lambda_2^{he}$ is positive for both cases, and no imperfection-sensitivity is exhibited.

In view of the large buckling mode deflection at the maximum load point, the agreement between the analytical predictions and the numerical results is remarkably good.

Thus, in every example considered here in which bifurcation of the perfect plate has taken place in the plastic range, the "overall" postbifurcation behaviour of the perfect plate and the degree of imperfection sensitity of an imperfect plate has agreed with the predictions of the hypoelastic analysis in which unloading is neglected. This agreement has been achieved even though the numerical results clearly show that, in the immediate vicinity of the bifurcation point of the perfect plate, the hypoelastic analysis does not apply, since in this vicinity the effect of elastic unloading is dominant.

A number of the curves presented in Figs. 1–4 have also been computed numerically for the corresponding hypoelastic plates without elastic unloading, thus using the same assumptions as were the basis for the asymptotic results (25)–(29). For most of the imperfect plates the numerical results for the elastic-plastic and hypoelastic plates were identical, because elastic unloading did not occur, and even for the perfect plates little difference was found except in the neighborhood of the bifurcation point. Therefore, the attempt to estimate imperfection-sensitivity of elastic-plastic plates by considering corresponding hypoelastic plates is reasonable and only involves minor numerical errors. For the quite different problem of an elastic-plastic column with

Table 3. Comparison of asymptotic hypoelastic predictions and numerical results for elastic-plastic square plates. The numbers in the first column refer to in-plane boundary conditions

| | h/a | n | $\bar{\xi}$ | Asymptotic | | Numerical | |
|---|---|---|---|---|---|---|---|
| | | | | $\lambda_{max}/\lambda_c$ | $\xi_{max}$ | $\lambda_{max}/\lambda_c$ | $\xi_{max}$ |
| I | .035 | 10 | .01 | .88 | .21 | .93 | .24 |
| | | | .1 | .81 | .27 | .86 | .52 |
| II | .035 | 10 | .01 | .88 | .21 | .93 | .23 |
| | | | .1 | .81 | .27 | .84 | .51 |
| II | .035 | 3 | .01 | .96 | .23 | .97 | .53 |
| | | | .1 | .87 | .85 | .94 | > 2 |
| I | .031 | 10 | .01 | .98 | .39 | .97 | .41 |
| | | | .1 | .92 | .82 | .94 | .78 |
| II | .031 | 10 | .01 | .97 | .23 | .96 | .29 |
| | | | .1 | .86 | .48 | .88 | .68 |

an asymmetric cross-section a similar agreement with the corresponding hypoelastic column has been found numerically [16]. The fact that eqns (25)–(29) are lowest order asymptotic results seems to be a more important approximation for the present case than the approximation due to disregarding elastic unloading.

## REFERENCES


1. W. T. Koiter, Introduction to the post-buckling behaviour of flat plates. *Colloque sur le Comportement Postcritique des utilisées en Construction Metallique*, Liege, November 1962, pp. 17–35, Mémoires de la société Royale des Sciences de Liege, 5me série, tome VIII, fascicule 5 (1963).
2. J. Mayers and B. Budiansky, Analysis of behavior of simply supported flat plates compressed beyond the buckling load into the plastic range. NACS TN 3368 (1955).
3. H. Ohtsubo, A method of elastic-plastic analysis of largely deformed plate problems. *Advances in Computational Methods in Structural Mechanics and Design* (Edited by J. T. Oden), p. 439. University of Alabama Press (1972).
4. K. W. Neale, Effect of imperfections on the plastic buckling of rectangular plates. *J. Appl. Mech.* **42**, 115 (1975).
5. J. W. Hutchinson, Post-bifurcation behavior in the plastic range. *J. Mech. Phys. Solids* **21**, 163 (1973).
6. J. W. Hutchinson, Plastic buckling. *Advances in Applied Mechanics* (Edited by C. S. Yih), Vol. 14, p. 67, Academic Press, New York (1974).
7. W. T. Koiter, Over de stabiliteit van het elastisch evenwicht. Thesis, Delft, H. J. Paris, Amsterdam (1945). English Translation issued as NASA TT F-10, 833 (1967).
8. J. W. Hutchinson and B. Budiansky, Analytical and numerical study of the effects of initial imperfections on the inelastic buckling of a cruciform column. *Proc. IUTAM Symp. on Buckling of Structures*, Harvard University, June 1974. Springer-Verlag.
9. V. Tvergaard and A. Needleman, Mode interaction in an eccentrically stiffened elastic-plastic panel under compression. *Proc. IUTAM Symp. on Buckling of Structures*, Harvard University, June 1974. Springer-Verlag (to appear).
10. V. Tvergaard and A. Needleman, Buckling of eccentrically stiffened elastic-plastic panels on two simple supports or multiply supported. *Int. J. Solids Struct.* **11**, 647 (1975).
11. R. Hill, Bifurcation and uniqueness in non-linear mechanics of continua. *Problems of Continuum Mechanics*, p. 155. S.I.A.M. Philadelphia (1961).
12. J. W. Hutchinson, Imperfection-sensitivity in the plastic range. *J. Mech. Phys. Solids* **21**, 191 (1973).
13. T. Kawai, Finite element analysis of the geometrically non-linear problems. *Recent Advances in Matrix Methods of Structural Analysis and Design*, p. 383. University of Alabama Press (1971).
14. O. C. Zienkiewicz, *The Finite Element Method in Engineering Science*, 2nd Edn. McGraw-Hill, London (1971).
15. A. Needleman, Postbifurcation behavior and imperfection-sensitivity of elastic-plastic circular plates. *Int. J. Mech. Sci.* **17**, 1 (1975).
16. V. Tvergaard and A. Needleman, On the buckling of elastic-plastic columns with asymmetric cross-sections. *Int. J. Mech. Sci.* **17**, 419 (1975).
17. B. Budiansky, Theory of buckling and post-buckling behavior of elastic structures. *Advances in Applied Mechanics* (Edited by C. S. Yih), Vol. 14, p. 2. Academic Press, New York (1974).


## APPENDIX 1

*Asymptotic analysis with elastic unloading neglected*

Here, the postbuckling analysis for a hypoelastic plate will be presented. The starting point of the analysis is the principle of virtual work. In much of the analysis it is convenient to use the total form of this principle rather than the incremental form (13) and to express the external virtual work in terms of quantities associated with the prebifurcation solution,

$$\int_A [(N_{\alpha\beta} - N^0_{\alpha\beta})\delta e_{\alpha\beta} + M_{\alpha\beta}\delta\kappa_{\alpha\beta} + N_{\alpha\beta}(w_{,\alpha} + \bar{w}_{,\alpha})\delta w_{,\beta}]\,dA = 0 \tag{A1}$$

where $A$ is the area of the plate middle surface, and in (A1), and throughout this analysis, $()^0$denotes field quantities associated with the prebifurcation solution (18). The quantity $\bar{w}$ denotes the magnitude and form of the initial imperfection, while $w$ measures the additional lateral deflection. Attention is confined to imperfections in the shape of the bifurcation mode (20) so that $\bar{w} = \bar{\xi}\overset{(1)}{w}$.

In many respects, the present analysis parallels that given by Hutchinson and Budiansky [8]. As in [8], it is convenient to divide the analysis into several parts: (i) a regular perturbation analysis valid for $\lambda < \lambda_c$, (ii) a singular perturbation analysis valid for $\lambda$ near $\lambda_c$, and (iii) the matching of (i) and (ii).

However, before undertaking the analysis of an imperfect plate we consider a perfect plate ($\bar{\xi} = 0$). The prebifurcation solution is given by (18) and the variational equation governing bifurcation is readily found to be

$$\int_A [\overset{(1)}{N}_{\alpha\beta}\delta e_{\alpha\beta} + \overset{(1)}{M}_{\alpha\beta}\delta\kappa_{\alpha\beta} + N^c_{\alpha\beta}\overset{(1)}{w}_{,\alpha}\delta w_{,\beta}]\,dA = 0. \tag{A2}$$

Here,

$$\overset{(1)}{\sigma}_{\alpha\beta} = L^c_{\alpha\beta\gamma\delta}\overset{(1)}{\eta}_{\gamma\delta} \tag{A3}$$

where $()^c$ denotes quantities evaluated at $\lambda = \lambda_c$, $\overset{(1)}{()}$ denotes quantities associated with the eigenmode and $\overset{(1)}{N}_{\alpha\beta}$ and $\overset{(1)}{M}_{\alpha\beta}$ are obtained from (A3) by (12). Throughout this analysis it will be convenient to work with $\sigma_{\alpha\beta}$ and $\eta_{\alpha\beta}$ in the constitutive equation, while continuing to employ $N_{\alpha\beta}$, $M_{\alpha\beta}$, $E_{\alpha\beta}$ and $\kappa_{\alpha\beta}$ in the principle of virtual work.

The solution to this bifurcation problem is,

$$\overset{(1)}{u}_\alpha = 0, \qquad \overset{(1)}{N}_{\alpha\beta} = 0 \tag{A4}$$

while $\lambda_c$ and $\overset{(1)}{w}$ are given by (19) and (20), and apply for an elastic-plastic as well as for the corresponding hypoelastic material. In Hill's[11] terminology this hypoelastic material is called a "linear comparison solid".

For an elastic-plastic material unloading plays a crucial role in determining the post befurcation behaviour as shown by Hutchinson[6] and, for the problems considered here, the initial postbifurcation expansion is given by (24). On the other hand, for a hypoelastic material, the initial postbifurcation expansion takes the form

$$\lambda = \lambda_c + \lambda_1^{he}\xi + \lambda_2^{he}\xi^2 + \cdots \tag{A5a}$$

$$u_\alpha = u_\alpha^0 + \overset{(2)}{u}_\alpha\xi^2 + \overset{(3)}{u}_\alpha\xi^3 + \tag{A5b}$$

$$w = \overset{(1)}{w}\xi + \overset{(2)}{w}\xi^2 + \overset{(3)}{w}\xi^3 + \cdots \tag{A5c}$$

In (A5), the notation $\lambda_i^{he}$ has been employed in order to emphasize that (A5a) is valid only when the unloading branch of (4) is suppressed. Furthermore, due to the symmetry of the plate, it can be shown that $\lambda_1^{he} = 0$.

In order for the expansion parameter $\xi$ to be well defined it is necessary to ensure that the functions $\overset{(i)}{w}$, $i > 1$, are orthogonal to $\overset{(1)}{w}$. This orthogonality condition is taken to be

$$\int_A N^c_{\alpha\beta}\,\overset{(1)}{w}_{,\alpha}\,\overset{(i)}{w}_{,\beta}\,dA = 0 \qquad i > 1. \tag{A6}$$

The expansion for the strains is found by substituting (A5b) and (A5c) into (1)–(3) to obtain

$$\eta_{\alpha\beta} = e^0_{\alpha\beta} + \overset{(1)}{\eta}_{\alpha\beta}\xi + \overset{(2)}{\eta}_{\alpha\beta}\xi^2 + \overset{(3)}{\eta}_{\alpha\beta}\xi^3 + \cdots \tag{A7}$$

where

$$\overset{(1)}{\eta}_{\alpha\beta} = x_3\,\overset{(1)}{\kappa}_{\alpha\beta} \tag{A8a}$$

$$\overset{(2)}{\eta}_{\alpha\beta} = \overset{(2)}{e}_{\alpha\beta} + \frac{1}{2}\overset{(1)}{w}_{,\alpha}\overset{(1)}{w}_{,\beta} + x_3\,\overset{(2)}{\kappa}_{\alpha\beta} \tag{A8b}$$

$$\overset{(3)}{\eta}_{\alpha\beta} = \overset{(3)}{e}_{\alpha\beta} + \frac{1}{2}(\overset{(2)}{w}_{,\alpha}\overset{(1)}{w}_{,\beta} + \overset{(1)}{w}_{,\alpha}\overset{(2)}{w}_{,\beta}) + x_3\,\overset{(3)}{\kappa}_{\alpha\beta} \tag{A8c}$$

The expansion for the stresses is obtained from (A7) and the constitutive relation (4), with $(\,)'$ identified as $d(\,)/d\xi$. The loading branch of the tensor of moduli is expanded in a Taylor series about $\lambda_c$,

$$L_{\alpha\beta\gamma\delta} = L^c_{\alpha\beta\gamma\delta} + (\sigma_{\mu\nu} - \sigma^c_{\mu\nu})\frac{\partial L_{\alpha\beta\gamma\delta}}{\partial\sigma_{\mu\nu}}\bigg|_c + \frac{1}{2}(\sigma_{\mu\nu} - \sigma^c_{\mu\nu})(\sigma_{\rho\omega} - \sigma^c_{\rho\omega})\frac{\partial^2 L_{\alpha\beta\gamma\delta}}{\partial\sigma_{\mu\nu}\partial\sigma_{\rho\omega}}\bigg|_c. \tag{A9}$$

Here, the subscript "$c$" indicates that the moduli derivatives are evaluated at $\sigma^c_{\mu\nu}$. The expansion for the stresses takes the form

$$\sigma_{\alpha\beta} = \sigma^0_{\alpha\beta} + \overset{(1)}{\sigma}_{\alpha\beta}\xi + \overset{(2)}{\sigma}_{\alpha\beta}\xi^2 + \overset{(3)}{\sigma}_{\alpha\beta}\xi^3 + \cdots \tag{A10}$$

where $\overset{(1)}{\sigma}_{\alpha\beta}$ is given by (A3) and

$$\overset{(2)}{\sigma}_{\alpha\beta} = L^c_{\alpha\beta\gamma\delta}\,\overset{(2)}{\eta}_{\gamma\delta} + \overset{(2)}{D}_{\alpha\beta} \tag{A11a}$$

$$\overset{(3)}{\sigma}_{\alpha\beta} = L^c_{\alpha\beta\gamma\delta}\,\overset{(3)}{\eta}_{\gamma\delta} + \overset{(3)}{D}_{\alpha\beta} \tag{A11b}$$

$$\overset{(2)}{D}_{\alpha\beta} = \frac{1}{2}\overset{(1)}{\sigma}_{\mu\nu}\frac{\partial L_{\alpha\beta\gamma\delta}}{\partial\sigma_{\mu\nu}}\bigg|_c\,\overset{(1)}{\eta}_{\gamma\delta} \tag{A(11c)}$$

$$\overset{(3)}{D}_{\alpha\beta} = \frac{2}{3}\lambda_2^{he}\,\overset{(1)}{\sigma}_{\mu\nu}\frac{\partial L_{\alpha\beta\gamma\delta}}{\partial\sigma_{\mu\nu}}\bigg|_c\frac{de^0_{\gamma\delta}}{d\lambda}\bigg|_c + \frac{2}{3}\overset{(1)}{\sigma}_{\mu\nu}\frac{\partial L_{\alpha\beta\gamma\delta}}{\partial\sigma_{\mu\nu}}\bigg|_c\,\overset{(2)}{\eta}_{\gamma\delta} + \frac{1}{3}\lambda_2^{he}\frac{d\sigma_{\mu\nu}}{d\lambda}\bigg|_c\frac{\partial L_{\alpha\beta\gamma\delta}}{\partial\sigma_{\mu\nu}}\bigg|_c\,\overset{(1)}{\eta}_{\gamma\delta}$$
$$+\frac{1}{3}\overset{(2)}{\sigma}_{\mu\nu}\frac{\partial L_{\alpha\beta\gamma\delta}}{\partial\sigma_{\mu\nu}}\bigg|_c\,\overset{(1)}{\eta}_{\gamma\delta} + \frac{1}{6}\overset{(1)}{\sigma}_{\mu\nu}\overset{(1)}{\sigma}_{\rho\omega}\frac{\partial^2 L_{\alpha\beta\gamma\delta}}{\partial\sigma_{\mu\nu}\partial\sigma_{\rho\omega}}\bigg|_c\,\overset{(1)}{\eta}_{\gamma\delta} \tag{A11d}\dagger$$

Employing the expansions (A5), (A7) and (A10) in (A1) gives,

$$2\xi\int_A [\overset{(2)}{N}_{\alpha\beta}\delta e_{\alpha\beta} + \overset{(2)}{M}_{\alpha\beta}\delta\kappa_{\alpha\beta} + N^c_{\alpha\beta}\,\overset{(2)}{w}_{,\alpha}\delta w_{,\beta}]\,dA + 3\xi^2\int_A \Big[\overset{(3)}{N}_{\alpha\beta}\delta e_{\alpha\beta} + \overset{(3)}{M}_{\alpha\beta}\delta\kappa_{\alpha\beta} + \overset{(2)}{N}_{\alpha\beta}\,\overset{(1)}{w}_{,\alpha}\delta w_{,\beta}$$
$$+\frac{\lambda_2^{he}}{\lambda_c}N^c_{\alpha\beta}\,\overset{(1)}{w}_{,\alpha}\delta w_{,\beta} + N^c_{\alpha\beta}\,\overset{(3)}{w}_{,\alpha}\delta w_{,\beta}\Big]\,dA + \cdots = 0 \tag{A12}$$

†The moduli derivatives are given in Appendix 2.

With $\delta(\,)$ replaced by $\overset{(1)}{(\,)}$, and employing (A2) and (A6), (A12) simplifies to

$$3\xi^2 \int_A \left[ \overset{(3)}{M}_{\alpha\beta} \overset{(1)}{\kappa}_{\alpha\beta} + \overset{(2)}{N}_{\alpha\beta} \overset{(1)}{w}_{,\alpha} \overset{(1)}{w}_{,\beta} + \frac{\lambda_2^{he}}{\lambda_c} N^c_{\alpha\beta} \overset{(1)}{w}_{,\alpha} \overset{(1)}{w}_{\beta} \right] dA + \cdots = 0 \tag{A13}$$

From (A11b) and the orthogonality condition (A6), we obtain

$$\int_A \overset{(3)}{M}_{\alpha\beta} \overset{(1)}{\kappa}_{\alpha\beta}\, dA = \int_A \int_{-h/2}^{h/2} x_3 \overset{(3)}{D}_{\alpha\beta} \overset{(1)}{\kappa}_{\alpha\beta}\, dx_3 dA \tag{A14}$$

The two relations (A13) and (A14) determine $\lambda_2^{he}$ once $\overset{(2)}{u}_\alpha$ and $\overset{(2)}{w}$ are known. By orthogonality $\overset{(2)}{w}$ vanishes, and $\overset{(2)}{u}_\alpha$ is found by solving an auxilliary boundary value problem, namely

$$\int_A \overset{(2)}{N}_{\alpha\beta} \delta e_{\alpha\beta}\, dA = 0 \tag{A15}$$

where

$$\overset{(2)}{N}_{\alpha\beta} = hL^c_{\alpha\beta\gamma\delta} \overset{(2)}{E}_{\gamma\delta} + \int_{-h/2}^{h/2} \overset{(2)}{D}_{\alpha\beta}\, dx_3. \tag{A16}$$

Here, this boundary value problem is solved by the finite element method. The solution is straightforward since (A15) and (A16) result in a plane stress problem with a distributed load. The solution of this boundary value problem and, therefore, the value of $\lambda_2^{he}$ depends on the in-plane boundary condition, as shown in Table 2.

(i) *Regular perturbation analysis for* $\lambda < \lambda_c$. For an imperfect plate, lateral deflection begins to occur as soon as $\lambda$ deviates from zero and, initially, $\lambda$ is a monotonically increasing function of the amplitude of the lateral deflection. Here, the lowest order effect of a small imperfection ($\bar{\xi} \ll 1$) on this rising part of the $\lambda - \xi$ curve is obtained. We seek expansions of the form

$$\begin{aligned} w &= \tilde{w}, \qquad u_\alpha = u_\alpha^0 + \tilde{u}_\alpha \\ \eta_{\alpha\beta} &= e^0_{\alpha\beta} + \tilde{\eta}_{\alpha\beta}, \qquad \sigma_{\alpha\beta} = \frac{\lambda}{\lambda_c} \sigma^c_{\alpha\beta} + \tilde{\sigma}_{\alpha\beta} \end{aligned} \tag{A17}$$

where $(\sim)$ are the perturbations of the field quantities due to the presence of the imperfection and vanish at $\lambda = 0$. Since, the expansions (A17) apply while $\lambda$ is monotonically increasing, in this part of the analysis, $\lambda$ will be employed as the parameter characterizing the loading history. All equations are linearized so that products of perturbation quantities and products of $\bar{\xi}$ with perturbation quantities are neglected.

The strain-displacement eqns (1)–(3) give,

$$\tilde{\eta}_{\alpha\beta} = \tilde{e}_{\alpha\beta} + x_3 \tilde{\kappa}_{\alpha\beta}. \tag{A18}$$

The tensor of moduli $L_{\alpha\beta\gamma\delta}$ is expanded in a Taylor series about the fundamental stress state, $\sigma^0_{\alpha\beta}$, of the form

$$L_{\alpha\beta\gamma\delta} = L^0_{\alpha\beta\gamma\delta} + \left. \frac{\partial L_{\alpha\beta\gamma\delta}}{\partial \sigma_{\mu\nu}} \right|_0 (\sigma_{\mu\nu} - \sigma^0_{\mu\nu}) + \cdots \tag{A19}$$

where "0" denotes moduli and moduli derivatives evaluated at $\sigma^0_{\mu\nu}$.

The linearized expansion for $\tilde{\sigma}_{\alpha\beta}$ is found from (A17), (A18) and (A19) to be

$$\frac{d\tilde{\sigma}_{\alpha\beta}}{d\lambda} = L^0_{\alpha\beta\gamma\delta} \frac{d\tilde{\eta}_{\gamma\delta}}{d\lambda} + \left. \frac{\partial L_{\alpha\beta\gamma\delta}}{\partial \sigma_{\mu\nu}} \right|_0 \tilde{\sigma}_{\mu\nu} \frac{de^0_{\gamma\delta}}{d\lambda} \tag{A20}$$

The linearized principle of virtual work is

$$\int_A \left[ \tilde{N}_{\alpha\beta} \delta e_{\alpha\beta} + \tilde{M}_{\alpha\beta} \delta\kappa_{\alpha\beta} + \frac{\lambda}{\lambda_c} N^c_{\alpha\beta} \tilde{w}_{,\alpha} \delta w_{,\beta} + \frac{\lambda}{\lambda_c} \bar{\xi} N^c_{\alpha\beta} \overset{(1)}{w}_{,\alpha} \delta w_{,\beta} \right] dA = 0. \tag{A21}$$

We now exploit the fact that, for the problems considered here, there is a complete set of eigenfunctions of the form

$$\overset{(i)}{w} = h \sin \frac{i_1 \pi x_1}{a} \sin \frac{i_2 \pi x_2}{a}, \qquad i_1, i_2, = 1, 2, 3 \ldots \tag{A22}$$

These eigenfunctions are orthogonal in the sense of (A6). This implies

$$\int_A \frac{h^3}{12} L^c_{\alpha\beta\gamma\delta} \overset{(i)}{\kappa}_{\alpha\beta} \overset{(j)}{\kappa}_{\gamma\delta}\, dA = 0 \qquad i \neq j. \tag{A23}$$

However, in addition to (A23), the eigenfunctions satisfy a much stronger orthogonality condition. Let $C_{\alpha\beta\gamma\delta}$ be a fourth order tensor independent of $x_\alpha$ satisfying the orthotropy conditions

$$C_{\alpha\beta\gamma\delta} = C_{\beta\alpha\gamma\delta} = C_{\alpha\beta\delta\gamma}, \qquad C_{1112} = C_{2212} = \; = C_{1211} = C_{1222} = 0. \tag{A24}$$

Then, as may be verified by noting the orthogonality properties of the sine and consine

$$\int_A C_{\alpha\beta\gamma\delta} \overset{(i)}{\kappa}_{\alpha\beta} \overset{(j)}{\kappa}_{\gamma\delta} \, dA = 0, \qquad i \neq j. \tag{A25}$$

From (A20) it can be seen that, to the order considered here, the moduli relating $\sigma_{\alpha\beta}$ to the strain history remain orthotropic, that is, satisfy (A24). Next, $\tilde{w}$ is expanded in terms of the complete set of functions (A22) and the principle of virtual work is differentiated with respect to $\lambda$. With $\delta(\,)$ replaced by $\overset{(i)}{(\,)}$ and using (A6) this gives

$$\int_A \left[ \frac{d\tilde{M}_{\alpha\beta}}{d\lambda} \overset{(1)}{\kappa}_{\alpha\beta} + \frac{d\xi}{d\lambda} \frac{\lambda}{\lambda_c} N^c_{\alpha\beta} \overset{(1)}{w}_{,\alpha} \overset{(1)}{w}_{,\beta} + (\xi + \bar{\xi}) \frac{1}{\lambda_c} N^c_{\alpha\beta} \overset{(1)}{w}_{,\alpha} \overset{(1)}{w}_{,\beta} \right] dA = 0. \tag{A26}$$

Employing (A20), (A25) and adding

$$-\frac{d\xi}{d\lambda} \int_A [\overset{(1)}{M}_{\alpha\beta} \overset{(1)}{\kappa}_{\alpha\beta} + N^c_{\alpha\beta} \overset{(1)}{w}_{,\alpha} \overset{(1)}{w}_{,\beta}] dA = 0. \tag{A27}$$

we obtain,

$$\begin{aligned}
&(\lambda - \lambda_c) \frac{d\xi}{d\lambda} \int_A \left[ \frac{h^3}{12} \frac{L^c_{\alpha\beta\gamma\delta} - L^0_{\alpha\beta\gamma\delta}}{(\lambda_c - \lambda)} \overset{(1)}{\kappa}_{\alpha\beta} \overset{(1)}{\kappa}_{\gamma\delta} + \frac{1}{\lambda_c} N^c_{\alpha\beta} \overset{(1)}{w}_{,\alpha} \overset{(1)}{w}_{,\beta} \right] dA \\
&+ \xi \int_A \left[ \frac{\partial L_{\alpha\beta\gamma\delta}}{\partial \sigma_{\mu\nu}} \bigg|_0 \frac{\tilde{M}_{\mu\nu}}{\xi} \frac{de^0_{\gamma\delta}}{d\lambda} \overset{(1)}{\kappa}_{\alpha\beta} - \frac{h^3}{12} \frac{\partial L_{\alpha\beta\gamma\delta}}{\partial \sigma_{\mu\nu}} \bigg|_0 \frac{d\sigma^0_{\mu\nu}}{d\lambda} \overset{(1)}{\kappa}_{\alpha\beta} \overset{(1)}{\kappa}_{\gamma\delta} \right] dA \\
&+ \xi \int_A \left[ \frac{h^3}{12} \frac{\partial L_{\alpha\beta\gamma\delta}}{\partial \sigma_{\mu\nu}} \bigg|_0 \frac{d\sigma^0_{\mu\nu}}{d\lambda} \overset{(1)}{\kappa}_{\alpha\beta} \overset{(1)}{\kappa}_{\gamma\delta} + \frac{1}{\lambda_c} N^c_{\alpha\beta} \overset{(1)}{w}_{,\alpha} \overset{(1)}{w}_{,\beta} \right] dA \\
&+ \bar{\xi} \int_A \frac{1}{\lambda_c} N^c_{\alpha\beta} \overset{(1)}{w}_{,\alpha} \overset{(1)}{w}_{,\beta} \, dA = 0.
\end{aligned} \tag{A28}$$

From (A28), it can be seen that $\xi \to \infty$ as $\lambda \to \lambda_c$, and from (A20)

$$\lim_{\lambda \to \lambda_c} \frac{1}{\xi} \tilde{M}_{\alpha\beta} = \overset{(1)}{M}_{\alpha\beta}. \tag{A29}$$

Thus, we can write

$$\xi = \bar{\xi} \left( 1 - \frac{\lambda}{\lambda_c} \right)^{-\Psi} p(\lambda) \tag{A30}$$

where from (A28) $\Psi$ is found to be

$$\Psi = 1 + \frac{\beta_1}{\beta_2} \tag{A31}$$

$$\beta_1 = \int_A \left[ \frac{\partial L_{\alpha\beta\gamma\delta}}{\partial \sigma_{\mu\nu}} \bigg|_c \overset{(1)}{M}_{\mu\nu} \frac{de_{\gamma\delta}}{d\lambda} \bigg|_c \overset{(1)}{\kappa}_{\alpha\beta} - \frac{h^3}{12} \frac{\partial L_{\alpha\beta\gamma\delta}}{\partial \sigma_{\mu\nu}} \bigg|_c \frac{d\sigma^0_{\mu\nu}}{d\lambda} \bigg|_c \overset{(1)}{\kappa}_{\alpha\beta} \overset{(1)}{\kappa}_{\gamma\delta} \right] dA \tag{A32}$$

$$\beta_2 = \int_A \left[ \frac{1}{\lambda_c} N^c_{\alpha\beta} \overset{(1)}{w}_{,\alpha} \overset{(1)}{w}_{,\beta} + \frac{h^3}{12} \frac{\partial L_{\alpha\beta\gamma\delta}}{\partial \sigma_{\mu\nu}} \bigg|_c \frac{d\sigma^0_{\mu\nu}}{d\lambda} \bigg|_c \overset{(1)}{\kappa}_{\alpha\beta} \overset{(1)}{\kappa}_{\gamma\delta} \right] dA. \tag{A33}$$

The quantity $\beta_1$ vanishes for an elastic material, linear or nonlinear, as is easily seen by using the fact that then the moduli can be derived from a strain energy density. Thus for an elastic plate $\Psi = 1$.

Since $p(\lambda)$ remains finite at $\lambda_c$, (A30) can be substituted into (A28) and $p(\lambda)$ computed by a straightforward procedure. As $\lambda/\lambda_c \to 1$, (A30) can be rewritten in the form

$$\frac{\lambda}{\lambda_c} \sim 1 - (p(\lambda_c))^{1/\Psi} \left( \frac{\bar{\xi}}{\xi} \right)^{1/\Psi}. \tag{A34}$$

This expression, (A34), which holds on the rising part of the $\lambda - \xi$ curve, will be matched with an asymptotic expression valid near $\lambda = \lambda_c$ obtained in the next part of the analysis.

(ii) *Singular perturbation analysis for* $\lambda \simeq \lambda_c$. An asymptotic expression, valid for small $|\lambda - \lambda_c|$, $\xi$ and $\bar{\xi}$, is sought that accounts for the lowest order effect of an imperfection. Following Budiansky [17], the functional relation between $\lambda$, $\xi$ and $\bar{\xi}$ is constrained by the relation $\bar{\xi} = \alpha \xi^\gamma$, so that for $\gamma$ properly chosen, only integer powers of $\xi$ are needed in the expansion about $\lambda_c$ to account for the lowest order effect of the imperfection. Thus, we assume expansions of the form

$$\lambda = \lambda_c + \bar{\lambda}_2 \xi^2 + \cdots \tag{A35a}$$

$$w = \overset{(1)}{\bar{w}} \xi + \overset{(2)}{\bar{w}} \xi^2 + \overset{(3)}{\bar{w}} \xi^3 + \cdots \tag{A35b}$$

$$u_\alpha = u_\alpha^0 + \overset{(1)}{\bar{u}}_\alpha \xi + \overset{(2)}{\bar{u}}_\alpha \xi^2 + \overset{(3)}{\bar{u}}_\alpha \xi^3 + \cdots \tag{A35c}$$

$$\eta_{\alpha\beta} = \eta^0_{\alpha\beta} + \overset{(1)}{\bar{\eta}}_{\alpha\beta}\xi + \overset{(2)}{\bar{\eta}}_{\alpha\beta}\xi^2 + \overset{(3)}{\bar{\eta}}_{\alpha\beta}\xi^3 + \cdots \tag{A35d}$$

$$\sigma_{\alpha\beta} = \sigma^0_{\alpha\beta} + \overset{(1)}{\bar{\sigma}}_{\alpha\beta}\xi + \overset{(2)}{\bar{\sigma}}_{\alpha\beta}\xi^2 + \overset{(3)}{\bar{\sigma}}_{\alpha\beta}\xi^3 + \cdots \tag{A35e}$$

Here, barred quantities are functions of $\alpha$ and for a perfect plate ($\alpha = 0$), reduce to their unbarred counterparts (A5), (A7), (A10). In (A35a), $\bar{\lambda}_1^{he}$ has been assumed zero. This results in no loss in generality since the same result for the lowest order effect of the imperfection is obtained with $\bar{\lambda}_1^{he} \neq 0$[17].

By employing $\xi$ as the expansion variable in (A35) we are anticipating the result, to be verified subsequently, that $\overset{(1)}{\bar{w}} = \overset{(1)}{w}$. Furthermore, we require that $\overset{(i)}{\bar{w}}$, $i > 1$, be orthogonal to $\overset{(1)}{w}$ ($= \overset{(1)}{\bar{w}}$) in the sense of (A6).

The parameter characterizing the loading history is now taken to be $\xi$ and $(\,)'$ denotes the derivative with respect to $\xi$ with $\bar{\xi}$ fixed. The expansions for the strain and stress increments obtained from (A35d) and (A35e) are

$$\dot{\eta}_{\alpha\beta} = \mathcal{L}_1(\overset{(1)}{\bar{\eta}}_{\alpha\beta}) + \mathcal{L}_2(\bar{\lambda}_1^{he}\eta'^c_{\alpha\beta} + \overset{(2)}{\bar{\eta}}_{\alpha\beta})\,\xi + \mathcal{L}_3(\bar{\lambda}_3^{he}\eta'^c_{\alpha\beta} + \overset{(3)}{\bar{\eta}}_{\alpha\beta})\,\xi^2 + \cdots \tag{A36a}$$

$$\dot{\sigma}_{\alpha\beta} = \mathcal{L}_1(\overset{(1)}{\bar{\sigma}}_{\alpha\beta}) + \mathcal{L}_2(\bar{\lambda}_2^{he}\sigma'^c_{\alpha\beta} + \overset{(2)}{\bar{\sigma}}_{\alpha\beta})\,\xi + \mathcal{L}_3(\bar{\lambda}_3^{he}\sigma'^c_{\alpha\beta} + \overset{(3)}{\bar{\sigma}}_{\alpha\beta})\,\xi^2 + \cdots \tag{A36b}$$

where as in[8]

$$\mathcal{L}_i(\,) = i(\,) - \alpha\gamma(\,)_{,\alpha} \tag{A37}$$

and $(\,)'^c$ denotes $\mathrm{d}(\,)/\mathrm{d}\lambda$ evaluated at $\lambda_c$.

The stress increments are given in terms of the strain increments by expanding the tensor of moduli in a Taylor series about $\sigma^c_{\alpha\beta}$ as in (A9). The lowest order term is

$$\mathcal{L}_1(\overset{(1)}{\bar{\sigma}}_{\alpha\beta}) = L^c_{\alpha\beta\gamma\delta}\mathcal{L}_1(\overset{(1)}{\bar{\eta}}_{\gamma\delta}). \tag{A38}$$

The solution of (A38) is

$$\overset{(1)}{\bar{\sigma}}_{\alpha\beta} = L^c_{\alpha\beta\gamma\delta}\overset{(1)}{\bar{\eta}}_{\gamma\delta} \tag{A39}$$

*plus* the homogeneous solution of (A38). This homogeneous solution gives rise to a stress field that does not vanish with $\xi$. Since there is no such stress field in the solution obtained in part (i) of the analysis, matching determines that the constant multiplying the homogeneous solution is zero. Therefore, for convenience, here and subsequently such homogeneous solutions will be discarded.

Substituting (A39) and (A35) into the principle of virtual work and taking the limit as $\xi \to 0$, with $\gamma > 1$, gives

$$\overset{(1)}{\bar{u}}_\alpha = 0, \qquad \overset{(1)}{\bar{w}} = \overset{(1)}{w}. \tag{A40}$$

From (A36), (A9) and (A40) we obtain,

$$\mathcal{L}_2(\overset{(2)}{\bar{\sigma}}_{\alpha\beta}) = \mathcal{L}_2(L^c_{\alpha\beta\gamma\delta}\overset{(2)}{\bar{\eta}}_{\gamma\delta}) + \overset{(1)}{\sigma}_{\mu\nu}\frac{\partial L_{\alpha\beta\gamma\delta}}{\partial\sigma_{\mu\nu}}\bigg|_c \overset{(1)}{\eta}_{\gamma\delta} \tag{A41}$$

$$\begin{aligned}\mathcal{L}_3(\overset{(3)}{\bar{\sigma}}_{\alpha\beta}) = {} & \mathcal{L}_3(L^c_{\alpha\beta\gamma\delta}\overset{(3)}{\bar{\eta}}_{\gamma\delta}) + \bar{\lambda}_2^{he}\sigma'^c_{\mu\nu}\frac{\partial L_{\alpha\beta\gamma\delta}}{\partial\sigma_{\mu\nu}}\bigg|_c \overset{(1)}{\eta}_{\gamma\delta} + \overset{(1)}{\sigma}_{\nu\nu}\frac{\partial L_{\alpha\beta\gamma\delta}}{\partial\sigma_{\mu\nu}}\bigg|_c \mathcal{L}_2(\bar{\lambda}_2^{he}e'^c_{\gamma\delta} + \overset{(2)}{\bar{\eta}}_{\gamma\delta}) \\ & + \overset{(2)}{\bar{\sigma}}_{\mu\nu}\frac{\partial L_{\alpha\beta\gamma\delta}}{\partial\sigma_{\mu\nu}}\bigg|_c \overset{(1)}{\eta}_{\gamma\delta} + \frac{1}{2}\overset{(1)}{\sigma}_{\mu\nu}\overset{(1)}{\sigma}_{\rho\omega}\frac{\partial^2 L_{\alpha\beta\gamma\delta}}{\partial\sigma_{\mu\nu}\partial\sigma_{\rho\omega}}\bigg|_c \overset{(1)}{\eta}_{\gamma\delta}.\end{aligned} \tag{A42}$$

Introducing $\Delta\lambda_2 = \bar{\lambda}_2^{he} - \lambda_2^{he}$, $\Delta\overset{(2)}{\sigma}_{\alpha\beta} = \overset{(2)}{\bar{\sigma}}_{\alpha\beta} - \overset{(2)}{\sigma}_{\alpha\beta}$ etc., into (A41) and (A42) and using (A11) we obtain

$$\mathcal{L}_2(\Delta\overset{(2)}{\sigma}_{\alpha\beta}) = \mathcal{L}_2(L^c_{\alpha\beta\gamma\delta}\Delta\overset{(2)}{\eta}_{\gamma\delta}) \tag{A43}$$

$$\begin{aligned}\mathcal{L}_3(\Delta\overset{(3)}{\sigma}_{\alpha\beta}) = {} & \mathcal{L}_3(L^c_{\alpha\beta\gamma\delta}\Delta\overset{(3)}{\eta}_{\gamma\delta}) + \overset{(1)}{\sigma}_{\mu\nu}\frac{\partial L_{\alpha\beta\gamma\delta}}{\partial\sigma_{\mu\nu}}\bigg|_c \mathcal{L}_2(\Delta\lambda_2 e'^c_{\gamma\delta} + \Delta\overset{(2)}{\eta}_{\gamma\delta}) \\ & + \Delta\lambda_2\sigma'^c_{\mu\nu}\frac{\partial L_{\alpha\beta\gamma\delta}}{\partial\sigma_{\mu\nu}}\bigg|_c \overset{(1)}{\eta}_{\gamma\delta} + \Delta\overset{(2)}{\sigma}_{\mu\nu}\frac{\partial L_{\alpha\beta\gamma\delta}}{\partial\sigma_{\mu\nu}}\bigg|_c \overset{(1)}{\eta}_{\gamma\delta}.\end{aligned} \tag{A44}$$

With the homogeneous solution discarded, (A43) gives

$$\Delta\overset{(2)}{\sigma}_{\alpha\beta} = L^c_{\alpha\beta\gamma\delta}\Delta\overset{(2)}{\eta}_{\gamma\delta}, \qquad \Delta\overset{(2)}{\eta}_{\alpha\beta} = \Delta\overset{(2)}{e}_{\alpha\beta} + x_3\Delta\overset{(2)}{\kappa}_{\alpha\beta}. \tag{A45}$$

Anticipating that $\gamma \geq 3$, the principle of virtual work gives

$$\int_A [\Delta\overset{(2)}{N}_{\alpha\beta}\delta e_{\alpha\beta} + \Delta\overset{(2)}{M}_{\alpha\beta}\delta\kappa_{\alpha\beta} + N^c_{\alpha\beta}\Delta\overset{(2)}{w}_{,\alpha}\delta w_{,\beta}]\,\mathrm{d}A = 0. \tag{A46}$$

Then, from (A2) and the orthogonality condition (A6), we obtain

$$\Delta \overset{(2)}{u}_\alpha = 0 \qquad \Delta \overset{(2)}{w} = 0. \tag{A47}$$

Thus, (A44) simplifies to

$$\mathscr{L}_3(\Delta \overset{(3)}{\sigma}_{\alpha\beta}) = \mathscr{L}_3(L^c_{\alpha\beta\gamma\delta}\Delta \overset{(3)}{\eta}_{\gamma\delta}) + \overset{(1)}{\sigma}_{\mu\nu}\frac{\partial L_{\alpha\beta\gamma\delta}}{\partial \sigma_{\mu\nu}}\bigg|_c \mathscr{L}_2(\Delta\lambda_2 e'^c_{\gamma\delta}) + \Delta\lambda_2 \sigma'^c_{\mu\nu}\frac{\partial L_{\alpha\beta\gamma\delta}}{\partial \sigma_{\mu\nu}}\bigg|_c \overset{(1)}{\eta}_{\gamma\delta}. \tag{A48}$$

The solution to this equation is

$$\Delta \overset{(3)}{\sigma}_{\alpha\beta} = L^c_{\alpha\beta\gamma\delta}\Delta \overset{(3)}{\eta}_{\gamma\delta} + \Delta\lambda_2 \sigma'^c_{\mu\nu}\frac{\partial L_{\alpha\beta\gamma\delta}}{\partial \sigma_{\mu\nu}}\bigg|_c \overset{(1)}{\eta}_{\gamma\delta} + \alpha^{3/\gamma}\left[\overset{(1)}{\sigma}_{\mu\nu}\frac{\partial L_{\alpha\beta\gamma\delta}}{\partial \sigma_{\mu\nu}}\bigg|_c e'^c_{\gamma\delta} - \sigma'^c_{\mu\nu}\frac{\partial L_{\alpha\beta\gamma\delta}}{\partial \sigma_{\mu\nu}}\bigg|_c \overset{(1)}{\eta}_{\gamma\delta}\right] \times \int^\alpha \alpha^{-1/\gamma}\frac{\mathrm{d}(\Delta\lambda_2\alpha^{-2/\gamma})}{\mathrm{d}\alpha}\mathrm{d}\alpha \tag{A49}$$

where the lower limit of the integral with respect to $\alpha$ is left unspecified temporarily.

The next terms of interest in the expansion of the principle of virtual work are

$$\xi^3 \int_A \left[\Delta \overset{(3)}{N}_{\alpha\beta}\delta e_{\alpha\beta} + \Delta \overset{(3)}{M}_{\alpha\beta}\delta\kappa_{\alpha\beta} + \frac{\Delta\lambda_2}{\lambda_c} N^c_{\alpha\beta}\overset{(1)}{w}_{,\alpha}\delta w_{,\beta}\right]\mathrm{d}A + \alpha\xi^\gamma \int_A N^c_{\alpha\beta}\overset{(1)}{w}_{,\alpha}\delta w_{,\beta}\,\mathrm{d}A + \cdots = 0. \tag{A50}$$

We will proceed on the assumption that $\gamma > 3$ and comment later on the case $\gamma = 3$. Substituting (A49) into (A50) and replacing $\delta()$ by $\overset{\cdot}{()}$ gives

$$\Delta\lambda_2 + (\Psi - 1)\alpha^{3/\gamma}\int^\alpha \alpha^{-1/\gamma}\frac{\mathrm{d}(\Delta\lambda_2\alpha^{-2/\gamma})}{\mathrm{d}\alpha}\mathrm{d}\alpha = 0 \tag{A51}$$

where $\Psi$ is given by (A31).

Multiplying (A51) by $\alpha^{-3/\gamma}$ and differentiating with respect to $\alpha$ yields,

$$\frac{\mathrm{d}(\Delta\lambda_2)}{\mathrm{d}\alpha} = \frac{2\Psi + 1}{\alpha(\gamma\Psi)}\Delta\lambda_2 \tag{A52}$$

Thus,

$$\Delta\lambda_2 = c\alpha^{(2\Psi+1/\gamma\Psi)}. \tag{A53}$$

Both $c$ and $\gamma$ are determined by matching (A35a) with (A34).

Before proceeding with this matching, the lower limit of the integral appearing in (A49) and (A51) will be specified. Call this lower limit $\alpha_0$ and substitute (A53) into (A51) to obtain

$$c\alpha^{3/\gamma}\alpha_0^{(1-\Psi)/\Psi\gamma} = 0. \tag{A54}$$

Since $\Psi$ is not less than one and $\gamma \geq 3$, $\alpha_0$ must be $\infty$.

(iii) *Matching.* When (A35a) and (A53) are rewritten in terms of $\xi$ and $\bar{\xi}$ using $\alpha = \bar{\xi}\xi^{-\gamma}$, the expansion for $\lambda$, valid for $|\lambda - \lambda_c|$ small, takes the form

$$\lambda = \lambda_c + \lambda_2^{he}\xi^2 + \frac{c\bar{\xi}^{(2\Psi+1)/\gamma\Psi}}{\xi^{1/\Psi}} + \cdots \tag{A55}$$

Let $\xi \to 0$, so that $|\lambda_2^{he}|\xi^2$ is small compared to the third term of (A55), which itself must be small for (A55) to be valid, then (A55) and (A34) give

$$c = -\lambda_c(p(\lambda_c))^{1/\Psi}, \qquad \gamma = 2\Psi + 1. \tag{A56}$$

Since $\Psi \geq 1$, with equality holding only if the hypoelastic material is actually elastic, (A56) implies $\gamma > 3$ if the material is not elastic. In the latter case (A50) yields a linear inhomogeneous algebraic equation for $\Delta\lambda_2$. In particular when $\lambda_c < \sigma_y$, the result for a linear elastic structure is obtained (see e.g. [17]).

## APPENDIX 2

*Moduli derivatives*

Here, the expressions for the derivatives of the tensor of moduli (11) employed in the postbuckling analysis will be given. The tensor of moduli (11) may be written in the form

$$L_{\alpha\beta\gamma\delta} = L^e_{\alpha\beta\gamma\delta} - g^{-1}m_{\alpha\beta}m_{\gamma\delta} \tag{B1}$$

where $L^e_{\alpha\beta\gamma\delta}$ is the linear elastic tensor of plane stresses moduli and

$$\hat{g} = \frac{1+\nu}{E}\left[\frac{2}{3}\frac{1+\nu}{E/E_t - 1} + 1\right] \tag{B2a}$$

$$g = \hat{g} - \frac{1}{6}\frac{1+\nu}{E}\frac{1-2\nu}{1-\nu}\frac{\sigma_{\gamma\gamma}^2}{\sigma_e^2} \tag{B2b}$$

$$m_{\alpha\beta} = \sqrt{\left(\frac{3}{2}\right)}\sigma_e^{-1}\left[\sigma_{\alpha\beta} - \frac{1}{3}\frac{1-2\nu}{1-\nu}\sigma_{\gamma\gamma}\delta_{\alpha\beta}\right]. \tag{B3}$$

Thus,

$$\frac{\partial L_{\alpha\beta\gamma\delta}}{\partial\sigma_{\mu\nu}} = -\frac{\partial g^{-1}}{\partial\sigma_{\mu\nu}}m_{\alpha\beta}m_{\gamma\delta} - g^{-1}\frac{\partial m_{\alpha\beta}}{\partial\sigma_{\mu\nu}}m_{\gamma\delta} - g^{-1}m_{\alpha\beta}\frac{\partial m_{\gamma\delta}}{\partial\sigma_{\mu\nu}} \tag{B4}$$

$$\begin{aligned}\frac{\partial^2 L_{\alpha\beta\gamma\delta}}{\partial\sigma_{\mu\nu}\partial\sigma_{\rho\omega}} = &-\frac{\partial^2 g^{-1}}{\partial\sigma_{\mu\nu}\partial\sigma_{\rho\omega}}m_{\alpha\beta}m_{\gamma\delta} - \frac{\partial g^{-1}}{\partial\sigma_{\mu\nu}}m_{\alpha\beta}\frac{\partial m_{\gamma\delta}}{\partial\sigma_{\rho\omega}}\\ &-\frac{\partial g^{-1}}{\partial\sigma_{\mu\nu}}\frac{\partial m_{\alpha\beta}}{\partial\sigma_{\rho\omega}}m_{\gamma\delta} - g^{-1}\frac{\partial m_{\alpha\beta}}{\partial\sigma_{\mu\nu}}\frac{\partial m_{\gamma\delta}}{\partial\sigma_{\rho\omega}} - g^{-1}\frac{\partial^2 m_{\alpha\beta}}{\partial\sigma_{\mu\nu}\partial\sigma_{\rho\omega}}m_{\gamma\delta} - \frac{\partial g^{-1}}{\partial\sigma_{\rho\omega}}\frac{\partial m_{\alpha\beta}}{\partial\sigma_{\mu\nu}}m_{\gamma\delta}\\ &-g^{-1}\frac{\partial m_{\alpha\beta}}{\partial\sigma_{\rho\omega}}\frac{\partial m_{\gamma\delta}}{\partial\sigma_{\mu\nu}} - g^{-1}m_{\alpha\beta}\frac{\partial^2 m_{\gamma\delta}}{\partial\sigma_{\mu\nu}\partial\sigma_{\rho\omega}} - \frac{\partial g^{-1}}{\partial\sigma_{\rho\omega}}m_{\alpha\beta}\frac{\partial m_{\gamma\delta}}{\partial\sigma_{\mu\nu}}.\end{aligned} \tag{B5}$$

Here,

$$\frac{\partial m_{\alpha\beta}}{\partial\sigma_{\mu\nu}} = \sqrt{\left(\frac{3}{2}\right)}\sigma_e^{-1}\left[\delta_{\alpha\mu}\delta_{\beta\nu} - \frac{1}{3}\frac{1-2\nu}{1-\nu}\delta_{\alpha\beta}\delta_{\mu\nu}\right] - m_{\alpha\beta}\sigma_e^{-1}\frac{\partial\sigma_e}{\partial\sigma_{\mu\nu}} \tag{B6}$$

$$\frac{\partial\sigma_e}{\partial\sigma_{\mu\nu}} = \frac{3}{2}\sigma_e^{-1}\left[\sigma_{\mu\nu} - \frac{1}{3}\sigma_{\gamma\gamma}\delta_{\mu\nu}\right] \tag{B7}$$

$$\frac{\partial g}{\partial\sigma_{\mu\nu}} = \left[\frac{\mathrm{d}\hat{g}}{\mathrm{d}\sigma_e}\frac{\partial\sigma_e}{\partial\sigma_{\mu\nu}} - \frac{1}{3}\frac{(1-2\nu)(1+\nu)}{(1-\nu)E}\frac{\sigma_{\gamma\gamma}}{\sigma_e^2}\delta_{\mu\nu} + \frac{1}{3}\frac{(1-2\nu)(1+\nu)}{(1-\nu)E}\frac{\sigma_{\gamma\gamma}^2}{\sigma_e^3}\frac{\partial\sigma_e}{\partial\sigma_{\mu\nu}}\right] \tag{B8}$$

$$\begin{aligned}\frac{\partial^2 m_{\alpha\beta}}{\partial\sigma_{\mu\nu}\partial\sigma_{\rho\omega}} = &-\sqrt{\left(\frac{3}{2}\right)}\sigma_e^{-2}\frac{\partial\sigma_e}{\partial\sigma_{\rho\omega}}\left[\delta_{\alpha\mu}\delta_{\beta\nu} - \frac{1}{3}\frac{1-2\nu}{1-\nu}\delta_{\alpha\beta}\delta_{\mu\nu}\right]\\ &-\frac{m_{\alpha\beta}}{\sigma_e}\frac{\partial^2\sigma_e}{\partial\sigma_{\mu\nu}\partial\sigma_{\rho\omega}} - \sigma_e^{-1}\frac{\partial m_{\alpha\beta}}{\partial\sigma_{\rho\omega}}\frac{\partial\sigma_e}{\partial\sigma_{\mu\nu}} + \sigma_e^{-2}\frac{\partial\sigma_e}{\partial\sigma_{\mu\nu}}\frac{\partial\sigma_e}{\partial\sigma_{\rho\omega}}m_{\alpha\beta}\end{aligned} \tag{B9}$$

$$\frac{\partial^2\sigma_e}{\partial\sigma_{\mu\nu}\partial\sigma_{\rho\omega}} = -\sigma_e^{-1}\frac{\partial\sigma_e}{\partial\sigma_{\mu\nu}}\frac{\partial\sigma_e}{\partial\sigma_{\rho\omega}} + \frac{3}{2}\sigma_e^{-1}\left[\delta_{\mu\rho}\delta_{\nu\omega} - \frac{1}{3}\delta_{\mu\nu}\delta_{\rho\omega}\right] \tag{B10}$$

$$\begin{aligned}\frac{\partial^2 g}{\partial\sigma_{\mu\nu}\partial\sigma_{\rho\omega}} = &\frac{\mathrm{d}^2\hat{g}}{\mathrm{d}\sigma_e^2}\frac{\partial\sigma_e}{\partial\sigma_{\mu\nu}}\frac{\partial\sigma_e}{\partial\sigma_{\rho\omega}} + \frac{\mathrm{d}\hat{g}}{\mathrm{d}\sigma_e}\frac{\partial^2\sigma_e}{\partial\sigma_{\mu\nu}\partial\sigma_{\rho\omega}}\\ &+\frac{(1+\nu)(1-2\nu)}{3E(1-\nu)}\left[-\sigma_e^{-2}\delta_{\mu\nu}\delta_{\rho\omega} + 2\sigma_e^{-3}\sigma_{\gamma\gamma}\frac{\partial\sigma_e}{\partial\sigma_{\rho\omega}}\delta_{\mu\nu}\right.\\ &\left.+2\sigma_e^{-2}\sigma_{\gamma\gamma}\frac{\partial\sigma_e}{\partial\sigma_{\mu\nu}}\delta_{\rho\omega} - 3\sigma_e^{-4}\sigma_{\gamma\gamma}^2\frac{\partial\sigma_e}{\partial\sigma_{\mu\nu}}\frac{\partial\sigma_e}{\partial\sigma_{\rho\omega}} + \sigma_e^{-3}\sigma_{\gamma\gamma}^2\frac{\partial^2\sigma_e}{\partial\sigma_{\mu\nu}\partial\sigma_{\rho\omega}}\right].\end{aligned} \tag{B11}$$